Available online at www.sciencedirect.com
ScienceDirect
Journal of Sound and Vibration 317 (2008) 419–431
JOURNAL OF SOUND AND VIBRATION
www.elsevier.com/locate/jsvi

Review

An analysis of longitudinal vibration of bimodular rod via smoothing function approach

Haitian Yang, Bin Wang*

Department of Engineering Mechanics, State Key Lab of Structural Analysis for Industrial Equipment, Dalian University of Technology, Dalian 116024, PR China

Received 6 May 2006; received in revised form 3 December 2007; accepted 29 March 2008
Handling Editor: L.G. Tham
Available online 19 May 2008

Abstract

This paper presents a new approach to solve dynamic bimodular problems. By utilizing a smoothing technique, the constitutive discontinuity can be avoided, and a FE-based precise incremental dynamic equation is derived. In order to secure the dynamic analysis credible, both a step-by-step linear acceleration algorithm and Wilson-θ method are employed in the solution process. Numerical verification gives satisfactory results.

Contents

1. Introduction

Both natural and synthetic materials exhibit a phenomenon known as bimodularity, i.e. the elastic properties in extension differ from those in compression. This phenomenon has been experimentally demonstrated in fiber glass-reinforced plastics, porcelain, rock, bone, concrete and composites, etc. [1]. The stress–strain behavior of such material is actually nonlinear, and is often approximated by a straight line with

*Corresponding author.
E-mail address: wangbin@student.dlut.edu.cn (B. Wang).

0022-460X/$ - see front matter
doi:10.1016/j.jsv.2008.03.060

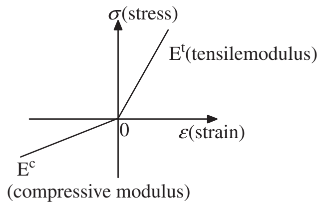

Fig. 1. An illustration of bimodular constitutive relationship.

a slope discontinuity at the origin, as shown in Fig. 1. This kind of material is referred to as the bimodular material.

Since Amartsumyan [1] proposed a set of fundamental constitutive equations for bimodular materials, fruitful achievement has been obtained in the study on static bimodular problems. Especially due to the constitutive discontinuity, analytical solutions are difficult to obtain in general, and numerical techniques have therefore been developed. By exploiting FEM and iterative techniques, bimodular bending problems of thick beam, thick plates, composite laminates, and layered composite structures were investigated by Tran [2], Chen [3–9], Srinivasan [10], Tsing [11], and Zinno [12]. However, in several of these papers, sufficient details regarding to the iterative process were not there. Zhang [13] employed FEM to investigate isotropic bimodular materials with numerical examples of plane problems. He [14] also compared solutions of $\mu^t/E^t \neq \mu^c/E^c$ with those of $\mu^t/E^t = \mu^c/E^c$. Yang [15] developed a FEM-based initial stress technique to solve two-dimensional (2-D) and 3-D static bimodular problems. A shape optimization of suspended bimodular insulator was realized by Zhao and Zhang [16] who used a sequential linear programming method in the optimizing process.

There are a number of reports investigating dynamic behaviors of bimodular composite plates. The solutions for this kind of nonlinear and non-smooth problems depend on the determination of the position of the unknown neutral surface. Lucchesi and Pagni considered the longitudinal vibration of an infinite prismatic bimodular rod, and proved that unique solution always exists except for the special case of no-tension material [17]. The dynamic responses of bimodular material, as Yang [18] illustrated in his report where a step-by-step integral method was presented to solve multi-degree bimodular vibration problems, is quite different from those of uni-modular elastic materials. Thereby it is practically and theoretically significant to make deeper investigation on this field.

The constitutive discontinuity and nonlinearity caused by bimodularity are the dominating difficulties in the dynamic analysis. One of the effective tools to deal with the discontinuity is the smoothing technique [19] by which a new precise incremental computing formula is derived in the dynamic bimodular analysis in this paper, and the variation of stiffness at a time interval can be taken into account. For the cases of one and two-degrees of freedom bimodular systems, in comparison with analytical and Wilson-θ method based solutions, the proposed approach is numerically verified with satisfactory results. A longitudinal vibration of a bimodular rod is investigated via the proposed algorithm and FEM. All the advantages of the proposed algorithm are illustrated in the context.

2. Constitutive relationship

The constitutive relationship of bimodular materials are defined by [1]

$$\{\varepsilon_I\} = [A(\sigma_I)]\{\sigma_I\} = [D]^{-1}\{\sigma_I\} \tag{1}$$

where $\{\varepsilon_I\} = \{\varepsilon_1, \varepsilon_2\ \varepsilon_3\}^{\mathrm{T}}$ and $\{\sigma_I\} = \{\sigma_1, \sigma_2, \sigma_3\}^{\mathrm{T}}$ denote principal strain and stress, respectively.

$$[A(\sigma_I)] = \begin{bmatrix} A_{11} & A_{12} & A_{13} \\ A_{21} & A_{22} & A_{23} \\ A_{31} & A_{32} & A_{33} \end{bmatrix} \tag{2}$$

$[D]$ is the inverse matrix of $[A]$

$$\begin{cases} A_{ii} = \frac{1}{E^t} & (\sigma_i > 0) \\ A_{ii} = \frac{1}{E^c} & (\sigma_i < 0) \end{cases} \quad (i = 1, 2, 3) \tag{3}$$

$$A_{ik} = -\frac{\mu^t}{E^t} \quad (\sigma_k > 0) \quad (i, k = 1, 2, 3, i \neq k)$$

$$A_{ik} = -\frac{\mu^c}{E^c} \quad (\sigma_k < 0) \quad (i, k = 1, 2, 3, i \neq k)$$

E^t and E^c stand for tensile and compressive moduli, respectively; μ^t and μ^c refer to tensile and compressive Poisson's ratios, respectively.

We assume [1] $-\mu^c/E^c = -\mu^t/E^t$. Eq. (3) can be described by a maximum or a minimum function, having the form

$$A_{ii} = \frac{\max\{0, \sigma_i\}}{|\sigma_i|} \frac{1}{E^t} + \frac{\max\{0, -\sigma_i\}}{|\sigma_i|} \frac{1}{E^c} \tag{4}$$

or

$$A_{ii} = \frac{1}{\sigma_i} \max\left\{\frac{\sigma_i}{E^t}, \frac{\sigma_i}{E^c}\right\}, \quad E^t < E^c \tag{5a}$$

$$A_{ii} = \frac{1}{\sigma_i} \min\left\{\frac{\sigma_i}{E^t}, \frac{\sigma_i}{E^c}\right\}, \quad E^t > E^c \tag{5b}$$

By smoothing maximum and minimum functions in Eqs. (4) and (5) [19], Eq. (2) can be rewritten as

$$[A] = \begin{bmatrix} f(\sigma_1) & c & c \\ c & f(\sigma_2) & c \\ c & c & f(\sigma_3) \end{bmatrix} \tag{6}$$

where $c = -(\mu^c/E^c) = -(\mu^t/E^t)$.

For Eq. (4)

$$f(\sigma_i) = \frac{1}{p} \ln(1 + e^{p\sigma_i}) \frac{1}{|\sigma_i|} \frac{1}{E^t} + \frac{1}{p} \ln(1 + e^{-p\sigma_i}) \frac{1}{|\sigma_i|} \frac{1}{E^c} \tag{7}$$

For Eq. (5a)

$$f(\sigma_i) = \frac{1}{\sigma_i} \frac{1}{p} \ln(e^{p\sigma_i/E^t} + e^{p\sigma_i/E^c}) \tag{8a}$$

For Eq. (5b)

$$f(\sigma_i) = -\frac{1}{\sigma_i} \frac{1}{p} \ln(e^{-p\sigma_i/E^t} + e^{-p\sigma_i/E^c}) \tag{8b}$$

$i = 1,2,3$.

The relationship between principal and general stresses is specified by [1]

$$\{\sigma\} = [T]\{\sigma_I\} \tag{9}$$

The relationship between principal and general strains is specified by [1]

$$\{\varepsilon_I\} = [T]^{\mathrm{T}}\{\varepsilon\} \tag{10}$$

Therefore

$$\{\sigma\} = [T][D][T]^{\mathrm{T}}\{\varepsilon\} = [D(\sigma)]\{\varepsilon\} \tag{11}$$

where $\{\sigma\}$and $\{\varepsilon\}$ designate vectors of the general stress and strain, respectively. $[T]$ is defined by

$$[T] = \begin{bmatrix} l_1^2 & m_1^2 & n_1^2 & l_1m_1 & m_1n_1 & n_1l_1 \\ l_2^2 & m_2^2 & n_2^2 & l_2m_2 & m_2n_2 & n_2l_2 \\ l_3^2 & m_3^2 & n_3^2 & l_3m_3 & m_3n_3 & n_3l_3 \end{bmatrix} \tag{12}$$

where l_i, m_i and n_i ($i = 1,2,3$) are the direction cosines, respectively.

In the one-dimensional case, we have

$$\sigma(\varepsilon) = \begin{cases} E^t\varepsilon & \varepsilon \geqslant 0 \\ E^c\varepsilon & \varepsilon \leqslant 0 \end{cases} \tag{13}$$

and

$$\sigma(\varepsilon) = \frac{1}{p}\ln(\mathrm{e}^{pE^t\varepsilon} + \mathrm{e}^{pE^c\varepsilon}) \tag{14}$$

Thus

$$\mathrm{d}\sigma = \frac{\partial\sigma}{\partial\varepsilon}\mathrm{d}\varepsilon = \frac{E^+\mathrm{e}^{pE^t\varepsilon} + E^-\mathrm{e}^{pE^c\varepsilon}}{\mathrm{e}^{pE^t\varepsilon} + \mathrm{e}^{pE^c\varepsilon}}\mathrm{d}\varepsilon \tag{15}$$

3. Incremental dynamic analysis for the vibration of a bimodular rod

Consider the longitudinal vibration of a bimodular rod, the governing equation is defined by

$$\frac{\partial\sigma}{\partial x} + F_V = \rho\frac{\partial^2 u}{\partial^2 t} + c\frac{\partial u}{\partial t} \tag{16}$$

where σ represents the stress, F_V stands for a body force, ρ refers to the mass density, u is displacement, and c designates a viscous damping coefficient.

The initial and boundary conditions are specified by

$$u_{t=0} = u_0 \tag{17}$$

$$\dot{u}_{t=0} = \dot{u}_0 \tag{18}$$

$$u_{x=0} = 0 \tag{19}$$

$$\bar{T} = A\sigma_{x=L} = P \tag{20}$$

where u_0 and $\dot{u}_0$ are prescribed functions, A refers to the area of cross section of the rod.

Utilizing an incremental virtual displacement principle, we have

$$\int_v \delta\varepsilon\Delta\sigma\mathrm{d}V = -\int_v \delta u\rho\Delta\ddot{u}\mathrm{d}V - \int_v \delta uc\Delta\dot{u}\mathrm{d}V + \int_v \delta u\Delta F_v\mathrm{d}V + \int_{S_\sigma} \delta u\Delta\bar{T}\mathrm{d}S \tag{21}$$

where δu represents the virtual displacement, and $\delta\varepsilon = (\partial/\partial x)\delta u$. Δu, $\Delta\dot{u}$ and $\Delta\ddot{u}$ can be evaluated by their nodal values via

$$\Delta u = [N]\{\Delta\bar{u}\} \tag{22}$$

$$\Delta\dot{u} = [N]\{\Delta\dot{\bar{u}}\} \tag{23}$$

$$\Delta\ddot{u} = [N]\{\Delta\ddot{\bar{u}}\} \tag{24}$$

where $[N]$ refers to a matrix of shape functions. $\{\Delta\bar{u}\}$, $\{\Delta\dot{\bar{u}}\}$ and $\{\Delta\ddot{\bar{u}}\}$ stand for nodal vectors of Δu, $\Delta\dot{u}$ and $\Delta\ddot{u}$:

$$\Delta\varepsilon = \frac{\partial}{\partial x}[N]\{\Delta\bar{u}\} = [B]\{\Delta\bar{u}\} \tag{25}$$

Substituting Eq. (15) and Eqs. (22)–(25) for Eq. (21) and interplating δu in the form of Eq. (22) then yields

$$[M]\{\Delta\ddot{u}\} + [C]\{\Delta\dot{u}\} + [K]\{\Delta u\} = \{\Delta f\} \tag{26}$$

where

$$[M] = \int_V \rho[N]^{\mathrm{T}}[N]\,\mathrm{d}v \tag{27}$$

$$[C] = \int_V c[N]^{\mathrm{T}}[N]\,\mathrm{d}v \tag{28}$$

$$[K] = \int_V [B]^{\mathrm{T}}\frac{\partial\sigma}{\partial\varepsilon}[B]\,\mathrm{d}v \tag{29}$$

$$\{\Delta f\} = \int_v [N]^{\mathrm{T}}\Delta F_v\,\mathrm{d}V + \int_{S_\sigma}[N]^{\mathrm{T}}\Delta\bar{T}\,\mathrm{d}S \tag{30}$$

$\{\Delta u\}, \{\Delta\dot{u}\}$ and $\{\Delta\ddot{u}\}$ are general nodal vectors of Δu, $\Delta\dot{u}$ and $\Delta\ddot{u}$, respectively.

The emphasis of this paper is to establish Eq. (26) in particular taking the constitutive discontinuity and the variation of stiffness with time into account. Actually one has variety options of numerical schemes for solving Eq. (26) [20], such as Wilson-θ method that is the extension of step-by-step linear acceleration algorithm to deal with nonlinear dynamic system, and serves to assure the numerical stability of the solution process regardless of the magnitude selected for the time step [21], and a step-by-step linear acceleration algorithm derived in the following:

At a discretized time interval we assume

$$\{u\} = \{c_0\} + \{c_1\}\xi + \{c_2\}\xi^2 + \{c_3\}\xi^3 \tag{31}$$

where $\xi = (t - t_0/\Delta t)$ and $\mathrm{d}\xi = \mathrm{d}t/\Delta t$.

Thus

$$\frac{\mathrm{d}\{u\}}{\mathrm{d}t} = \frac{\mathrm{d}\{u\}}{\mathrm{d}\xi}\frac{\mathrm{d}\xi}{\mathrm{d}t} = \frac{1}{\Delta t}\left[\{c_1\} + 2\{c_2\}\xi + 3\{c_3\}\xi^2\right] \tag{32}$$

$$\frac{\mathrm{d}^2\{u\}}{\mathrm{d}t^2} = \frac{\mathrm{d}}{\mathrm{d}t}\frac{\mathrm{d}\{u\}}{\mathrm{d}t} = \frac{1}{\Delta t^2}[2\{c_2\} + 6\{c_3\}\xi] \tag{33}$$

where Δt and t_0 denote the length and the start point of the time interval, respectively.

At the beginning of a time interval where $\xi = 0$:

$$\begin{aligned} \{c_0\} &= \{u\}_{\xi=0} \\ \{c_1\} &= \Delta t\{\dot{u}\}_{\xi=0} \\ \{c_2\} &= \Delta t^2\frac{\{\ddot{u}\}_{\xi=0}}{2} \end{aligned} \tag{34}$$

At the end of time interval where $\xi = 1$:

$$\{\Delta u\} = \{c_1\} + \{c_2\} + \{c_3\} \tag{35}$$

$$\{\Delta\dot{u}\} = \frac{1}{\Delta t}[2\{c_2\} + 3\{c_3\}] \tag{36}$$

$$\{\Delta\ddot{u}\} = \frac{1}{\Delta t^2}6\{c_3\} \tag{37}$$

By exploiting Eqs. (31)–(37), Eq. (26) can be written as

$$\frac{1}{\Delta t^2}6[M]\{c_3\} + \frac{1}{\Delta t}[C][2\{c_2\} + 3\{c_3\}] + [K][\{c_1\} + \{c_2\} + \{c_3\}] = \{\Delta f\} \tag{38}$$

The whole solution process consists of five steps:

1. Determine $\{u\}_{t=t_0}$ and $\{\dot{u}\}_{t=t_0}$. At the first time interval, $\{u\}_{t=t_0}$ and $\{\dot{u}\}_{t=t_0}$ are provided by initial conditions. At other time intervals, $\{u\}_{t=t_0}$ and $\{\dot{u}\}_{t=t_0}$ are given by

$$\begin{aligned} \{u\} &= \{c_0\} + \{c_1\} + \{c_2\} + \{c_3\} \\ \{\dot{u}\} &= \{c_1\} + 2\{c_2\} + 3\{c_3\} \end{aligned} \quad \text{(at the last time interval)}$$

2. Determine $\{\ddot{u}\}$ via $\{\ddot{u}\} = [M]^{-1}[[f] - [C]\{\dot{u}\} - [K]\{u\}]$.
3. Calculate $[C]$ and $[K]$.
4. Solve $\{c_0\}$,$\{c_1\}$,$\{c_2\}$ via Eq. (34), and obtain $\{c_3\}$ via Eq. (38).
5. Go to the next time interval, and repeat steps 1–4.

In order to secure the dynamic analysis credible, both the proposed step-by-step linear acceleration algorithm and Wilson-θ method are employed in the solution process, providing a numerical comparison.

4. Numerical verification

All computing parameters are assumed dimensionless for simplicity. Example 1 considers a free vibration of a one-degree of freedom bimodular system shown in Fig. 2 where $m = 3,\ C = 0,\ k^+ = 12\pi^2,\ k^- = 3\pi^2,\ u_0 = 0.2,\ \dot{u}_0 = 0$.

Numerical results are shown in Table 1 and compared with an analytical solution give by [15]

$$\begin{aligned} u_i^+ &= 0.2\sin\left(2\pi t + \frac{\pi}{2} - 3i\pi\pi\right), \quad i = 0,\ i = 1,2,3,\ldots \\ &\left(0 \leqslant t \leqslant \frac{1}{4}, \frac{5}{4} + (i-1)\frac{3}{2} \leqslant t \leqslant \frac{3}{2} + (i-1)\frac{3}{2}\right) \\ u_i^- &= -0.4\sin\left(\pi\pi - \frac{\pi}{4} - \frac{3(i-1)\pi}{2}\right), \quad i = 1,2,3\ldots \\ &\left(\frac{3}{2} + (i-1)\frac{3}{2} \leqslant t \leqslant \frac{5}{2} + (i-1)\frac{3}{2}\right) \end{aligned}$$

Example 2 considers the forced vibration of a same system as Example 1 with the same initial conditions. Other computing parameters are

$$m = 3,\ \ c = 3,\ \ k^+ = 12\pi^2,\ \ k^- = 3\pi^2,\ \ p = 15\sin\frac{\pi t}{2}$$

Fig. 3 gives a comparison of response and excitation. Numerical results are exhibited in Table 2 and compared with the solution given by Wilson-θ method.

Example 3 considers a two-degrees of freedom bimodular system shown in Fig. 4 where

$$k_1^+ = 3,\ \ k_1^- = 1,\ \ k_2^+ = 2,\ \ k_2^- = 1,\ \ \{u\}_{t=0} = \begin{Bmatrix} 0 \\ 0 \end{Bmatrix},\ \ \{\dot{u}\}_{t=0} = \begin{Bmatrix} 0 \\ 0 \end{Bmatrix},\ \ \{p\} = \begin{Bmatrix} 15 \\ 15 \end{Bmatrix}\sin \pi t,\ \ [M] = \begin{bmatrix} 5 & 0 \\ 0 & 3 \end{bmatrix}$$

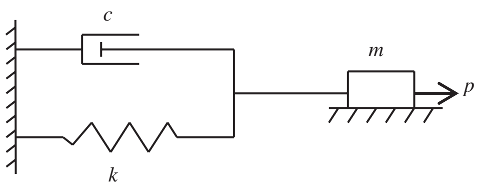

Fig. 2. An one-degree of freedom bimodular system.

Table 1
Numerical comparison of displacement in a free vibration

t/s	Analytical solution	Presented method	
		$\Delta t = 0.01$	$\Delta t = 0.005$
0	0.2	0.2	0.2
0.5	−0.282843	−0.279105	0.281064
1.0	−0.282843	−0.285861	−0.284421
1.5	0.2	0.199846	0.199962
2.0	−0.282843	−0.279	−0.281037
2.5	−0.282843	−0.285975	−0.284449
3.0	0.2	0.199841	0.199962
3.5	−0.282843	−0.278895	−0.28101
4.0	−0.282843	−0.286089	−0.284477
4.5	0.2	0.199835	0.199961
5.0	−0.282843	−0.278789	−0.280983
5.5	−0.282843	−0.286203	−0.284505
6.0	0.2	0.199829	0.19996
6.5	−0.282843	−0.278683	−0.280956
7.0	−0.282843	−0.286316	−0.284533
7.5	0.2	0.199823	0.19996
8.0	−0.282843	−0.278577	−0.280929
8.5	−0.282843	−0.28643	−0.28456
9.0	0.2	0.199817	0.199959
9.5	−0.282843	−0.278471	−0.280902
10.0	−0.282843	−0.286543	−0.284588

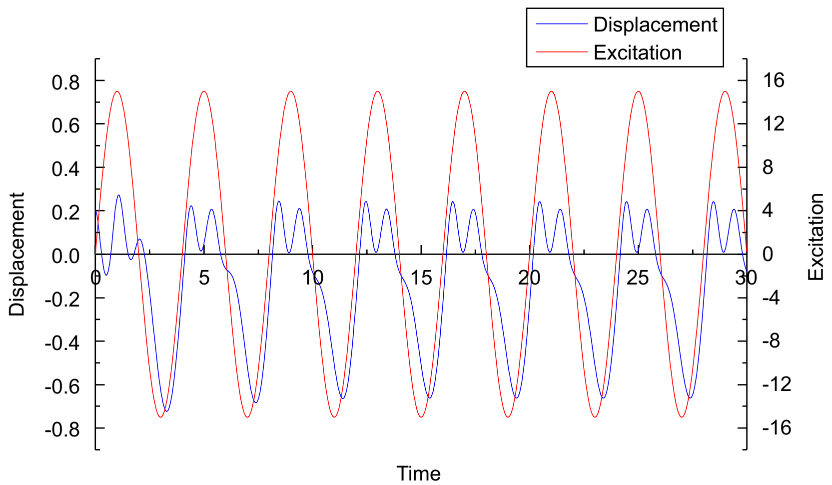

Fig. 3. The comparison of response and excitation.

Table 2
Numerical comparison of displacements in a forced vibration

t/s	Wilson-θ method		Presented method		
	$\Delta t = 0.01$	$\Delta t = 0.005$	$\Delta t = 0.01$	$\Delta t = 0.005$	$\Delta t = 0.001$
0	0.2	0.2	0.2	0.2	0.2
0.5	−0.0972883	−0.097013	−0.09647	−0.0965251	−0.0965449
1.0	0.257017	0.25702	0.257196	0.257161	0.257151
1.5	0.00507127	0.00494761	0.00472369	0.00474091	0.00474502
2.0	0.0658818	0.0658879	0.0666242	0.0666056	0.0665985
2.5	−0.175017	−0.17568	−0.176867	−0.176934	−0.176952
3.0	−0.619761	−0.620157	−0.620746	−0.620766	−0.620773
3.5	−0.665543	−0.665095	−0.664366	−0.664317	−0.664304
4.0	−0.157984	−0.157118	−0.156159	−0.156134	−0.156126
4.5	0.201507	0.201017	0.200792	0.20066	0.200625
5.0	0.047974	0.0485148	0.0488641	0.0490027	0.0490416
5.5	0.167856	0.167284	0.166941	0.166804	0.166765
6.0	−0.0669796	−0.0668546	−0.0666668	−0.0665429	−0.06651
6.5	−0.167901	−0.167995	−0.16797	−0.167869	−0.167839
7.0	−0.515436	−0.516083	−0.516725	−0.516814	−0.516839
7.5	−0.666588	−0.666507	−0.66651	−0.666572	−0.66659
8.0	−0.221304	−0.220289	−0.219323	−0.219256	−0.219237
8.5	0.237244	0.236788	0.236747	0.23658	0.236538
9.0	0.0203107	0.0208013	0.0211821	0.0213425	0.0213852
9.5	0.18921	0.188688	0.188323	0.188174	0.188133
10.0	−0.0827592	−0.0827558	−0.0827452	−0.0826455	−0.0826219

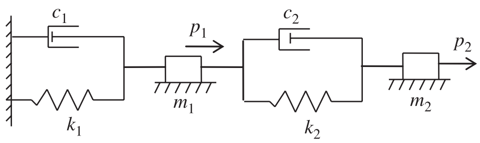

Fig. 4. A two-degree of freedom bimodular system.

Numerical results are listed in Tables 3 and 4, and compared with the solutions obtained by Wilson-θ method. Figs. 5 and 6 describe the variations of displacements of m_1 and m_2, respectively.

Example 4 considers the longitudinal vibration of a bimodular rod shown in Fig. 7 where $\rho = 1$, $C = 0$, $L = 10$, $A = 1$. Thirty quadratic elements with same size are employed in the FE analysis.

Table 5 gives a numerical results of free vibration with $E^t = E^c = 50$, and compared with an analytical solution [22]. The initial condition is specified by $\{u\}_{t=0} = 1, \{\dot{u}\}_{t=0} = 0$.

For the cases where $E^t = E^c = 50$; $E^t = 60$, $E^c = 50$; $E^t = 80$, $E^c = 50$; and $E^t = 100$, $E^c = 50$; Figs. 8a–d give the variations of displacements at $x = L$ with $\{u\}_{t=0}$ $\{\dot{u}\}_{t=0} = 0$ $\rho = 1$, $c = 1$, $L = 10$, $A = 1$, $P = 15\cos 2\pi t$. Table 6 gives a detailed comparison of the proposed step linear acceleration algorithm and Wilson-θ method in the term of the size of time step.

4.1. Computing remarks

1. The deformation behavior of bimodular problem strongly depends on the ratio of E^t/E^c It is definitely reasonable that if $E^c < E^t$, the compressive displacement will be larger than tensile one as shown in Figs. 3, 5 and 6, thereby for a given E^t the decrease of E^c will lead to the increase of the compressive displacement as shown in Figs. 8a–d. In this case if the compressive displacement gets large enough the movement is probably unable to return from a compressive state to the tensile

Table 3
Numerical comparison of displacement of m_1

t/s	Wilson-θ method		Presented method	
	$\Delta t = 0.01$	$\Delta t = 0.001$	$\Delta t = 0.01$	$\Delta t = 0.001$
0	0	0	0	0
0.5	0.17188	0.17263	0.17282	0.17284
1.0	0.92827	0.93364	0.93419	0.93427
1.5	1.6155	1.6193	1.6191	1.6192
2.0	1.5773	1.5723	1.5711	1.5713
2.5	1.4032	1.4031	1.4032	1.4033
3.0	1.7302	1.7368	1.7389	1.7391
3.5	1.9525	1.9501	1.9528	1.953
4.0	1.4287	1.4231	1.4268	1.4269
4.5	0.8014	0.80201	0.8071	0.80716
5.0	0.73831	0.73903	0.74359	0.74365
5.5	0.62899	0.62744	0.62985	0.6299
6.0	−0.13258	−0.13714	−0.13829	−0.13831
6.5	−0.90618	−0.91054	−1.6733	−0.91522
7.0	−1.073	−1.0703	−1.0771	−1.0772
7.5	−1.2195	−1.2202	−1.2292	−1.2293
8.0	−1.955	−1.9639	−1.9739	−1.974
8.5	−2.6782	−2.6794	−2.6871	−2.6873
9.0	−2.7415	−2.738	−2.7423	−2.7426
9.5	−2.73	−2.734	−2.7355	−2.7356
10.0	−3.2606	−3.265	−3.2624	−3.2627

Table 4
Numerical comparison of displacement of m_2

t/s	Wilson-θ method		Presented method	
	$\Delta t = 0.01$	$\Delta t = 0.001$	$\Delta t = 0.01$	$\Delta t = 0.001$
0	0	0	0	0
0.5	0.2869	0.28816	0.28832	0.28834
1.0	1.554	1.5629	1.5656	1.5657
1.5	2.7269	2.7335	2.7384	2.7386
2.0	2.7216	2.7136	2.7186	2.7189
2.5	2.5017	2.5019	2.5086	2.5088
3.0	3.1035	3.1147	3.1223	3.1226
3.5	3.506	3.5022	3.5069	3.5072
4.0	2.6342	2.6248	2.6274	2.6276
4.5	1.5462	1.5469	1.5493	1.5494
5.0	1.353	1.3537	1.3553	1.3554
5.5	1.0617	1.0586	1.0602	1.0603
6.0	−0.30797	−0.31605	−0.31244	−0.31248
6.5	−1.6736	−1.6811	−1.6733	−1.6735
7.0	−1.9787	−1.974	−1.9613	−1.9615
7.5	−2.1894	−2.1902	−2.1761	−2.1763
8.0	−3.3211	−3.3352	−3.3223	−3.3226
8.5	−4.3685	−4.3694	−4.3567	−4.3571
9.0	−4.26	−4.2528	−4.2427	−4.243
9.5	−4.0029	−4.0082	−4.004	−4.004
10.0	−4.6628	−4.669	−4.6698	−4.6703

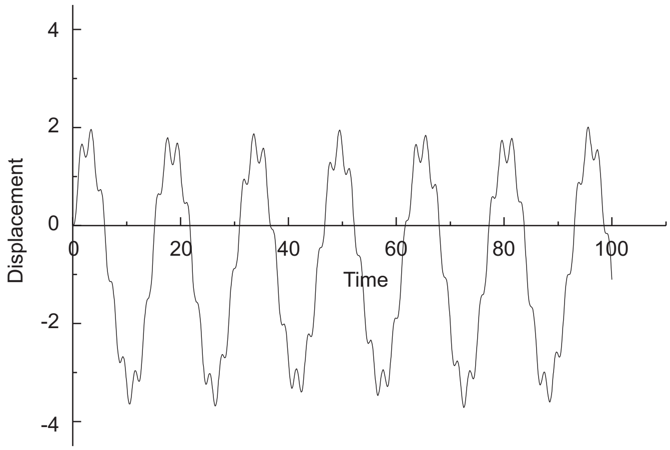

Fig. 5. The variation of displacement of m_1 with time.

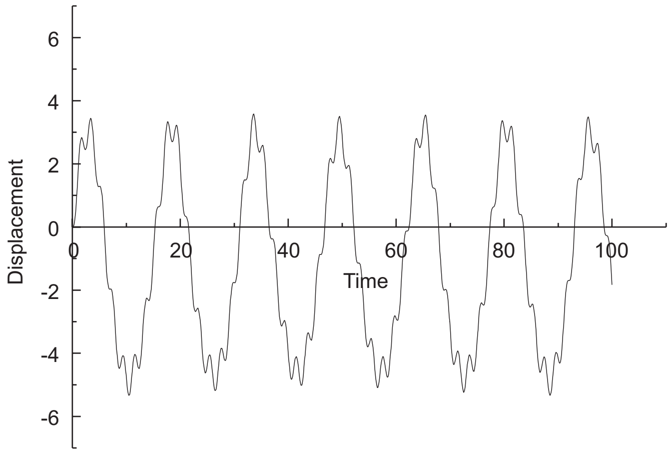

Fig. 6. The variation of displacement of m_2 with time.

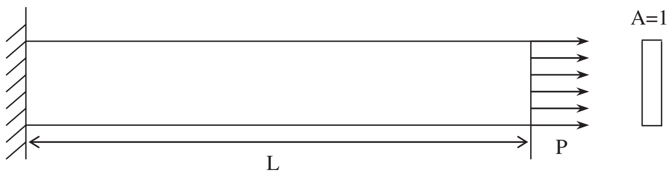

Fig. 7. A bimodular rod.

state in a load cycle, and eventually keeps 'compressive' at the steady stage of vibration as shown in Fig. 8d.

2. The comparison of displacements obtained by analytical solution, Wilson-θ method and the proposed step linear acceleration algorithm exhibits fairly good accordance as shown in Tables 2–6 and Figs. 8a–d, and provides a credible evidence of the overall approaches presented in this paper numerically. Both the proposed step linear acceleration algorithm and Wilson-θ method can be employed in the bimodular dynamical analysis. Since Wilson-θ method is able to assure the numerical stability of the solution process regardless of magnitude selected for the time step [20] it seems to be a more proper option.

Table 5
Numerical comparison of displacement at $x = L$ in a free vibration ($E^t = E^c = 50$)

t/s	Analytical solution	Presented method	
		$\Delta t = 0.01$	$\Delta t = 0.001$
0	1	1	1
0.1	0.899976	0.90053	0.8999
0.2	0.79998	0.79801	0.79995
0.3	0.699981	0.69836	0.69968
0.4	0.599983	0.59947	0.59955
0.5	0.499985	0.49894	0.50059
0.6	0.399988	0.39854	0.40044
0.7	0.299991	0.29975	0.30185
0.8	0.199994	0.20064	0.20119
0.9	0.0999968	0.10019	0.10215

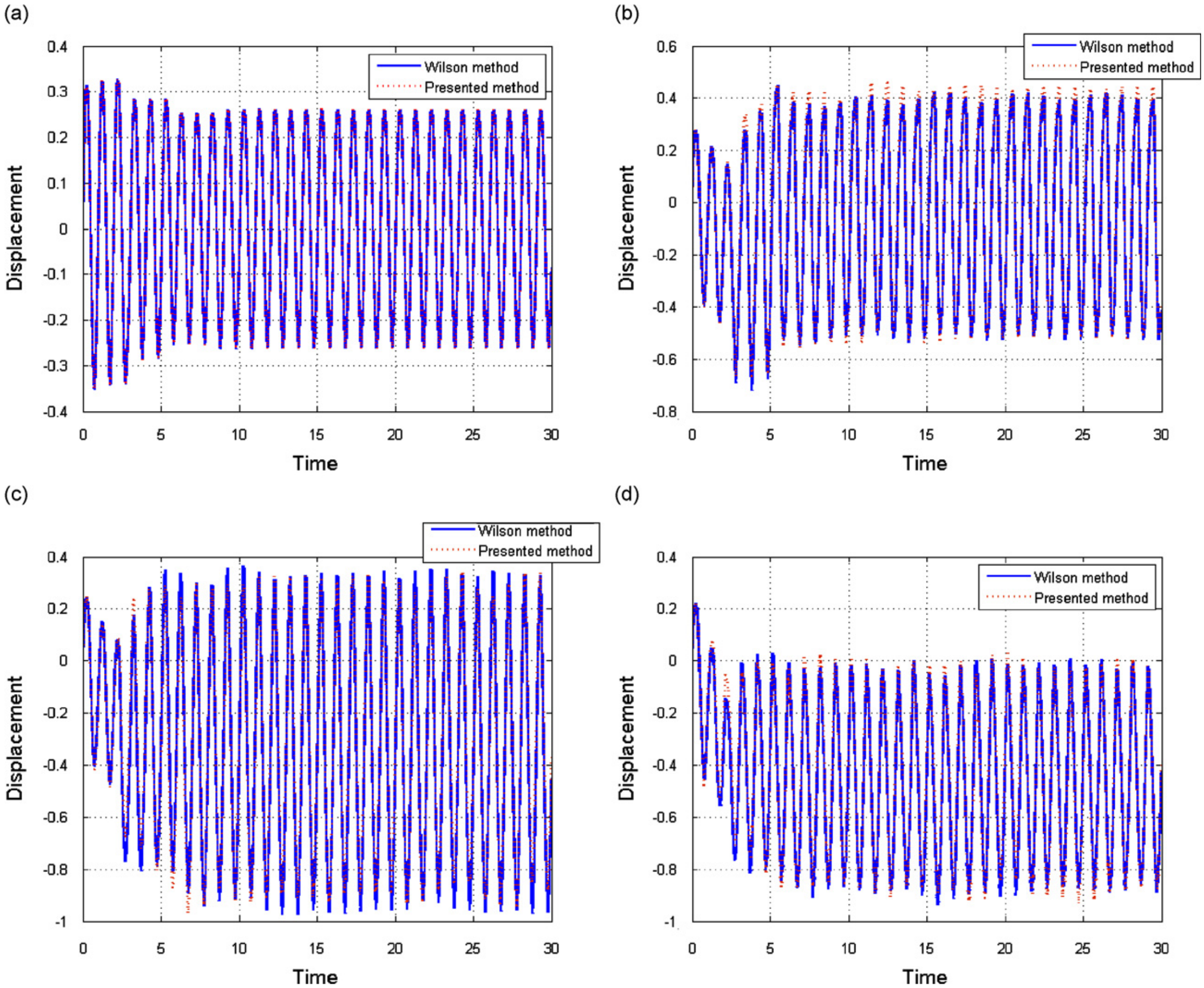

Fig. 8. (a) Displacement at $x = L$ ($E^t = E^c = 50$); (b) displacement at $x = L$ ($E^t = 60$, $E^c = 50$); (c) displacement at $x = L$ ($E^t = 80$, $E^c = 50$); (d) displacement at $x = L$ ($E^t = 100$, $E^c = 50$).

Table 6
Numerical comparison of displacements with different sizes of time step at $x = L$ ($E^t = 60$, $E^c = 50$)

t/s	$\Delta t = 0.001$		$\Delta t = 0.0005$		$\Delta t = 0.00025$		$\Delta t = 0.0001$	
	Wilson-θ	Presented	Wilson-θ	Presented	Wilson-θ	Presented	Wilson-θ	Presented
10.00	−0.398620	−0.392951	−0.393405	−0.392060	−0.392218	−0.391816	−0.391826	−0.391713
10.05	−0.269301	−0.263715	−0.264568	−0.262218	−0.262621	−0.261631	−0.261677	−0.261322
10.10	−0.111583	−0.105996	−0.106958	−0.104307	−0.104749	−0.103662	−0.103711	−0.103329
10.15	0.029482	0.035866	0.034717	0.037919	0.037356	0.038751	0.038685	0.039195
10.20	0.131238	0.137438	0.136292	0.139554	0.138988	0.140404	0.140340	0.140851
10.25	0.210798	0.217908	0.216599	0.219942	0.219303	0.220817	0.220736	0.221302
10.30	0.287999	0.294590	0.293209	0.296801	0.296087	0.297807	0.297715	0.298367
10.35	0.350175	0.357751	0.356408	0.359955	0.359312	0.360873	0.360797	0.361364
10.40	0.376424	0.386040	0.384240	0.389027	0.388113	0.390339	0.390225	0.391062
10.45	0.409544	0.419962	0.418375	0.422342	0.421660	0.423278	0.423205	0.423758
10.50	0.352343	0.350535	0.351315	0.349056	0.349495	0.348392	0.348451	0.348011
10.55	0.158909	0.157078	0.157940	0.155841	0.156316	0.155191	0.155261	0.154801
10.60	−0.051303	−0.051780	−0.051082	−0.052784	−0.052382	−0.053341	−0.053283	−0.053672
10.65	−0.234542	−0.235820	−0.235235	−0.236827	−0.236514	−0.237301	−0.237262	−0.237564
10.70	−0.383184	−0.384874	−0.384385	−0.385530	−0.385293	−0.385846	−0.385812	−0.386029
10.75	−0.480749	−0.481865	−0.481406	−0.482559	−0.482315	−0.482898	−0.482864	−0.483093
10.80	−0.547213	−0.547371	−0.547252	−0.547652	−0.547623	−0.547716	−0.547719	−0.547730
10.85	−0.548128	−0.546684	−0.546813	−0.546435	−0.546506	−0.546328	−0.546337	−0.546267
10.90	−0.527752	−0.526761	−0.526839	−0.526729	−0.526794	−0.526674	−0.526693	−0.526613
10.95	−0.488408	−0.484738	−0.485494	−0.483446	−0.483879	−0.482820	−0.482881	−0.482450
11.00	−0.406416	−0.398952	−0.400244	−0.396841	−0.397450	−0.395970	−0.396043	−0.395499

5. Concluding remarks

The major contributions of this paper include:

1. Making use of a smooth technique avoids inconveniences induced by the constitutive discontinuity.
2. In virtue of the smoothed constitutive equation, the variation of stiffness at a time interval can be taken into account, thereby a new precise incremental computing formula is derived in the dynamic bimodular analysis.
3. The verification of proposed approach is numerically fulfilled via one-degree and two-degrees of freedom systems, and a longitudinal vibration problem of a bimodular rod.

Acknowledgments

The research leading to this paper is funded by NSF (10421002), NSF (10472019), (10772035), NSF (10721062), NKBRSF [2005CB321704], and the fund of disciplines leaders of young and middle age faculty in colleges of Liaoning Province.

References

[1] S.A. Ambartsumyan, A.A. Khachatryan, The basic equations of the theory of elasticity for materials with different tensile and compressive stiffness, *Mechanics of Solids* 1 (1966) 29–34.
[2] A.D. Tran, C.W. Bert, Bending of thick beams of bimodulus materials, *Computers and Structures* 15 (6) (1982) 627–642.
[3] Ji-Liang Doong, Lien-Wen Chen, Axisymmetric vibration of an initially stressed bimodulus thick circular plate, *Journal of Sound and Vibration* 94 (4) (1984) 461–468.
[4] Ji-Liang Doong, Lien-Wen Chen, Vibration of a bimodulus thick plate, *Journal of Vibration Acoustic Stress Reliability Design* 107 (1) (1985) 92–97.

[5] Dar-Ping Juang, Lien-Wen Chen, Axisymmetric buckling of bimodulus thick circular plates, *Computers and Structures* 25 (2) (1987) 175–182.
[6] Lien-Wen Chen, Dar-Ping Juang, Axisymmetric vibration of bimodulus thick circular and annular plates, *Computers and Structures* 25 (5) (1987) 759–764.
[7] Lien-Wen Chen, Dar-Ping Juang, Axisymmetric dynamic stability of a bimodulus thick circular plate, *Computers and Structures* 26 (6) (1987) 933–939.
[8] Lien-Wen Chen, C.C. Chen, Asymmetric buckling of bimodulus thick annular plates, *Computers and Structures* 29 (6) (1988) 1063–1074.
[9] B.T. Jzeng, P.D. Lin, L.W. Chen, Dynamic stability of bimodulus thick plates, *Computers and Structures* 45 (4) (1992) 745–753.
[10] R.S. Srinivasan, L.S. Ramachandra, Bending of bimodulus annular plates, *Computers and Structures* 27 (2) (1987) 305–310.
[11] Yi-Ping Tseng, Cheng-Tao Lee, Bending analysis of bimodular laminates using a high-order finite strip method, *Composite Structures* 30 (1995) 341–350.
[12] Raffaele Zinno, Fabrizio Greco, Damage evolution in bimodular laminated composites under cyclic loading, *Composite Structures* 53 (2001) 381–402.
[13] Y.Z. Zhang, Z.F. Wang, The finite element method for elasticity with different moduli in tension and compression, *Computed Structural Mechanics and Application* 6 (1) (1989) 236–246.
[14] Y.Z. Zhang, Numerical method of bimodulus problem under condition of $\theta \neq 0$ and error analysis of supposing $\theta = 0$, *Journal of Dalian University of Technology* 34 (6) (1994) 641–645.
[15] H.T. Yang, R.F. Wu, Solution to problem of dual extension–compression elastic modulus with initial stress method, *Journal of Dalian University of Technology* 32 (1) (1992) 35–39.
[16] D.Z. Zhao, Y.Z. Zhang, Shape optimization of suspended insulator with dual elastic modulus, *Journal of Dalian University of Technology* 34 (1) (1992) 10–16.
[17] Massimiliano Lucchesi, Andrea Pagni, Longitudinal oscillations of bimodular rods, *International Journal of Structural Stability and Dynamics* 5 (1) (2005) 37–54.
[18] H.T. Yang, K.J. Yang, Dynamic analysis for the problem of dual extension-compression elastic modulus, *Computed Structural Mechanics and Application* 10 (4) (1993) 438–448.
[19] X.S. Li, An effective method for the non-differentiable optimization problems, *Science in China (Series A)* 24 (4) (1994) 373–377.
[20] P.A.Z. Mario, *Structural Dynamics—Theory and Computation*, VNR Company, New York, 1980.
[21] E.L. Wilson, et al., Nonlinear dynamic analysis of complex structures, *International Journal of Earthquake Engineering and Structural Dynamics* 1 (1973) 241–252.
[22] J.H. Lin, N.S. Qu, H.C. Sun, *Computational Structural Dynamics*, Higher Education Press of China, 1998, pp. 76–75.